JOURNAL OF CATALYSIS 74, 317–322 (1982)

Catalytic Properties and Activity of Rare-Earth Orthoferrites in Oxidation of Methanol

TSUYOSHI ARAKAWA, SHIN-ICHI TSUCHI-YA, AND JIRO SHIOKAWA

Department of Applied Chemistry, Faculty of Engineering, Osaka University, 2-1 Yamadaoka, Suita-shi, Osaka-fu, Japan

Received April 28, 1981; revised November 4, 1981

The catalytic properties and activity of $LnFeO_3$ (Ln = La–Gd) in the reaction of methanol oxidation have been studied. $LnFeO_3$ are antiferromagnetic compounds and except for $PrFeO_3$ are an n-type semiconductor. The activity was in the following order: Gd > Eu > Sm > Nd > Pr > La, where the activity was measured at a temperature at which a conversion of methanol to CO_2 and H_2O became 10%. The relative magnitude of covalency for Fe–O bond in $LnFeO_3$ is determined with the measurement of the binding energy of Fe $2p_{3/2}$ in X-ray photoelectron spectra at 380°C and decreased as the radius of the rare-earth ion decreases. Further, from the measurement of reaction kinetics and conductivity, the mechanism was proposed.

INTRODUCTION

Some of the perovskite-type oxides show high electric conductivity and exhibit oxidation–reduction catalytic characteristics. Especially rare-earth cobaltites have been suggested as substitutes for noble metals in electrocatalysis and in automotive-exhaust catalysis (*1–3*), while an interesting aspect of rare-earth perovskites ($LnMO_3$) is that one is able to vary the dimensions of the unit cell by varying the lanthanide ion. Changes in the crystal dimensions may be expected to produce variations in the Ln–O and M–O interactions. It would be interesting, therefore, to study the effect of the rare-earth ion on the catalytic activity of rare-earth transition-metal mixed oxides.

We have studied the effect of the rare-earth ion on the catalytic properties of the rare-earth copper double oxides (*4–5*), the rare-earth manganites (*6*), and the rare-earth cobaltites in an attempt to obtain a gas sensor (*7*). In this report we mainly describe the relationship between the catalytic activity and the covalency of Fe–O bond in $LnFeO_3$.

EXPERIMENTAL PROCEDURES

The catalysts were prepared by the solid-state reaction of dried Ln_2O_3 and Fe_2O_3. The well-ground mixtures of components were fired at 1300°C in air for 10 hr. These compounds consisted of a single orthorhombic phase, as determined by X-ray diffraction (Table 1). Their BET surface area was smaller than about 2 m^2/g in all cases.

The magnetic-susceptibility data for $LnFeO_3$ were obtained with a Shimadzu MB-11 magnetic balance over the range 300–800 K.

Oxidation of methanol was carried out by the conventional flow method. The gaseous mixture (60 cm^3/min) of methanol (6 vol%) and O_2 (9 vol%), diluted with N_2 (85 vol%), was passed through the catalyst bed for 2 hr or more at reaction temperatures until the steady state was reached. A fixed contact time was usually 1 $g \cdot s/cm^3$. Then the gas composition was analyzed before and after the reaction by gas chromatography using the following column packing: Molecular sieve 13 X for N_2 and O_2, Porapak Q for CO_2, and Chromosorb 105 for CH_3OH.

0021-9517/82/040317-06$02.00/0

TABLE 1

X-Ray Lattice Constants for $LnFeO_3$

Catalyst	Symmetry	*a* (Å)	*b* (Å)	*c* (Å)
$LaFeO_3$	Orthorhombic	5.556	5.565	7.862
$PrFeO_3$	Orthorhombic	5.495	5.578	7.810
$NdFeO_3$	Orthorhombic	5.441	5.573	7.753
$SmFeO_3$	Orthorhombic	5.394	5.592	7.711
$EuFeO_3$	Orthorhombic	5.371	5.611	7.686
$GdFeO_3$	Orthorhombic	5.346	5.616	7.668

An X-ray photoemission study was performed by a Shimadzu 650 B ESCA spectrometer using Mg$K\alpha$ (1253.6 eV) radiation in the main spectrometer chamber (pressure $<10^{-8}$ Torr). We used a sintered pellet which was fired at 800°C in dry air for 1 hr, and immediately loaded onto the sample holder under argon atmosphere and pushed into an antechamber (pressure $<10^{-5}$ Torr). The spectra were subsequently recorded at 25 and 380°C. A calibration of the binding energy was accomplished using a C 1*s* electron line (285.0 eV) coming from the background. The measured energies were consistent within ±0.1 eV.

The thin oxide film of $GdFeO_3$ for electrical measurement was prepared using a procedure similar to that reported previously (*8*). The thin film was set in a Pyrex glass tube and the gaseous mixture (40 cm^3/min) of N_2 (100-*X* vol%) and O_2 (*X* vol%) was passed through. Methanol (1 μl) was introduced at an injection port. The conductivity changes due to the presence of methanol were recorded as a source of direct current; a dc voltage generator (10 V) was used. The electric current flowing through the thin film was measured with an electric recorder as the potential drop across a fixed resistance (400 Ω) to be connected in series with the thin film.

RESULTS AND DISCUSSION

Catalytic Properties of $LnFeO_3$

The catalytic properties of $LnFeO_3$ are shown in Table 2. The property of the semiconductor for $LnFeO_3$, except for $PrFeO_3$, is n-type. That of $PrFeO_3$ moves from a p-type to an n-type. Except for $PrFeO_3$, the conductivity changes of chemisorption for methanol in nitrogen gas stream, as shown in a previous paper (*8*), correspond to the Seebeck coefficients at experimental temperature, while, $LnFeO_3$ are antiferromagnetic compounds and have a high Néel temperature T_N that increases with increasing radius of the rare-earth ion. Treves (*9*) has pointed out that the strength of the magnetic interaction decreases with decreasing lattice parameter because of the decreasing cation–anion–cation (Fe^{3+}–O^{2-}–Fe^{3+}) angle.

Measurement of Catalytic Activity

The catalytic activity of $LnFeO_3$ for methanol–O_2 reaction was tested over a wide range of temperature. The fraction of methanol converted at a fixed contact time was taken as a measure of the catalytic activity. The reaction products were CO_2 and H_2O. X-Ray powder diffraction patterns of catalysts measured before and after the reaction confirmed that there was no

TABLE 2

Catalytic Properties of $LnFeO_3$

Catalyst	Change of electrical conductivity	Seebeck coefficient (mV/K)	Néel temperature (K)
$LaFeO_3$	+	−0.30 (640–770 K)	708
$PrFeO_3$	+	+0.08–−0.02 (800–1000 K)	678
$NdFeO_3$	+	−0.22 (720–770 K)	665
$SmFeO_3$	+	−0.42 (710–770 K)	630
$EuFeO_3$	+	−0.40 (680–770 K)	624
$GdFeO_3$	+	−1.60–−2.20 (690–770 K)	617

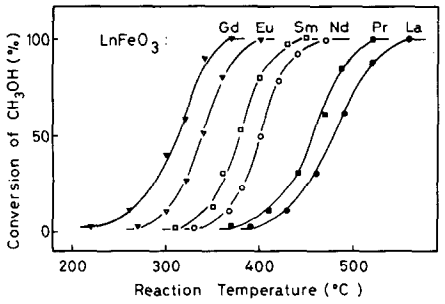

FIG. 1. Catalytic activity of $LnFeO_3$ (Ln = La–Gd) for the methanol oxidation reaction. Flow rate: CH_3OH, 3.6 cm^3/min; O_2, 5.4 cm^3/min; N_2, 51.0 cm^3/min. Contact time: 1 g · s/cm^3.

detectable loss in crystallinity. Figure 1 shows the conversion of methanol to products at various temperatures. The sequence of the activity was Gd > Eu > Sm > Nd > Pr > La for $LnFeO_3$, where the activity is given by the temperature at which the conversion of methanol attains 10%. Thus it is found that the activity for $LnFeO_3$ increases as the radius of the rare-earth ion decreases.

X-Ray Photoemission Measurement of $LnFeO_3$

The composition of the surface of the catalyst was investigated by ESCA. The Fe/Ln, Fe/O, and Ln/O ratios for orthoferrites are obtained by the measurement of the surface area for Fe(2*p*), Ln(4*d*), and O(1*s*) in the observed ESCA spectra. The Fe(2*p*)/O(1*s*), Ln(4*d*)/O(1*s*), and Fe(2*p*)/Ln(4*d*) intensity ratios are summarized in Table 3. The calculated values are based on the relative intensities of X-ray-induced photoelectron signals given by Jørgensen and Berthou (*10*). Since the observed values are consistent with the calculated values, it is suggested that the composition of a surface for a catalyst is close to that of a bulk.

The binding energy of Fe $2p_{3/2}$ at 25°C scarcely varies from compound to compound (Table 3). When catalyst was heated at 380°C, however, the binding energy became greater down the rare-earth series in $LnFeO_3$.

Successively, the change of the covalency of Fe–O bond in $LnFeO_3$ was estimated from the change in the binding energy of Fe $2p_{3/2}$. Chemical shift measurements have been made on numerous occasions, and the following equation has been used to describe them (*11*):

$$\Delta E_B = k\Delta q_N + \Delta V, \qquad (1)$$

where ΔE_B is the change in binding energy, k is a constant approximately equal to e^2/r (r = atomic radius), Δq_N is the change in the calculated atomic charge, and ΔV is the change in the crystal potential. ΔV can be written as an expression including a Madelung constant B,

$$\Delta V = \Delta q_N e^2 NB(1/R_i - 1/R_0), \qquad (2)$$

where e is the electron charge, R_i a nearest-neighbor Fe–O distance in $LnFeO_3$, R_0 a

TABLE 3

Intensity Ratio and Binding Energies of Photoelectron Peaks of $LnFeO_3$

Catalyst	Fe(2*p*)/O(1*s*)		Ln(4*d*)/O(1*s*)		Fe(2*p*)/Ln(4*d*)		Fe $2p_{3/2}$ (eV)		Δq_N
	Obsd	Calcd	Obsd	Calcd	Obsd	Calcd	25°C	380°C	
$LaFeO_3$	1.0	1.0	0.5	0.6	1.8	1.8	711.1_5	711.2_5	0
$PrFeO_3$	1.0	1.0	0.2	0.2	4.6	4.5	711.2	711.3	0.22
$NdFeO_3$	1.0	1.0	0.3	0.3	3.7	3.6	711.3	711.4_5	0.40
$SmFeO_3$	1.0	1.0	0.4	—	2.3	—	711.2	711.6	0.54
$EuFeO_3$	1.0	1.0	0.4	0.4	2.3	2.3	711.4	711.7	0.66
$GdFeO_3$	1.0	1.0	0.5	0.4	2.2	2.3	711.3	711.8	0.72

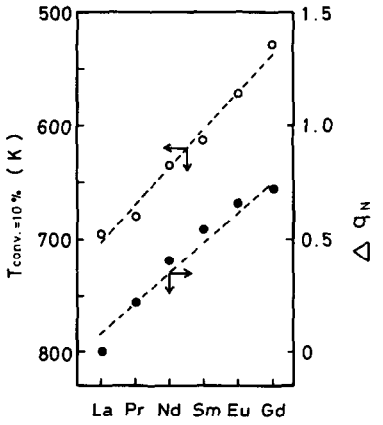

FIG. 2. Relative catalytic activity and covalency of Fe–O bond against the rare-earth element in $LnFeO_3$.

nearest-neighbor Fe–O distance in $LaFeO_3$, and N Avogadro's number. Thus, on the basis of $LaFeO_3$, Δq_N is calculated (see Table 3). Δq_N increases with decreasing radius of rare-earth ion. Carver *et al.* (*12*) have observed that the binding energy of Fe $2p_{3/2}$ in FeF_3 (q_N = 2.11) and $FeCl_3$ (q_N = 0.91) is 714.4 and 711.5 eV, respectively; namely, Fe $2p_{3/2}$ shifts to higher binding energy as the ionic property of Fe–X (X = halogen ion) bond becomes large. Therefore, it will be noted that the ionic property of Fe–O bond becomes large down the rare-earth series in $LnFeO_3$.

The pattern of relative catalytic activities against the rare-earth element in $LnFeO_3$ is shown in Fig. 2, compared with the relative covalency of Fe–O bond in $LnFeO_3$. The activity increases as the covalency of Fe–O bond decreases down the rare-earth series.

Mechanism of Oxidation of Methanol

We discussed the mechanism of oxidation of methanol on $LnFeO_3$ with the kinetic and conductivity data. Figure 3 shows the dependence of the rate of the CH_3OH–O_2 reaction for $GdFeO_3$ upon the partial pressures of reactant gases, P_{CH_3OH} and P_{O_2}, at 300°C. The reaction order was unity in P_{CH_3OH} and 0.5 in P_{O_2}. The equation which represents the experimental data is

$$r = -\frac{dP_{CH_3OH}}{dt} = kP_{CH_3OH}P_{O_2}^{0.5}. \quad (3)$$

On the other hand, the conductivity change of $GdFeO_3$ due to the injection of 1 μl methanol is shown in Fig. 4. After the injection of methanol, the conductivity increases immediately and then is restored to its initial value. The magnitude of conductivity change decreases with increasing oxygen concentration in carrier gas up to 2.0 vol% of oxygen concentration which reacts stoichiometrically with the amount of pulsed methanol. Then, the conductivity change is extremely small above 2.0 vol% of oxygen concentration. In these cases the reaction products in outlet gases were CO_2 and H_2O.

On the basis of these experimental results of the activity, kinetics, and conduc-

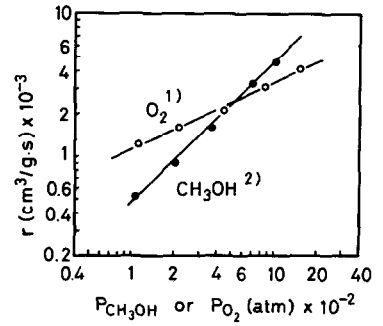

FIG. 3. Dependence of the rate of the CH_3OH–O_2 reaction on the partial pressures of O_2 at P_{CH_3OH} = 0.06 atm (1) and of CH_3OH at P_{O_2} = 0.09 atm (2).

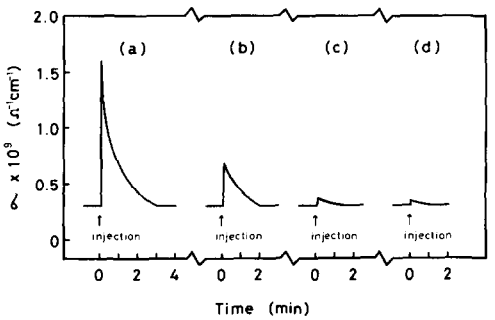

FIG. 4. The variation of conductivity (σ) of $GdFeO_3$ after the injection of CH_3OH as a function of time at 350°C. The concentration of oxygen in carrier gas (40 cm^3/min) is: (a) 0.5 vol%, (b) 1.0 vol%, (c) 2.0 vol%, (d) 10.0 vol%.

tivity data, we tentatively propose that methanol oxidation occurs between O_2 and CH_3OH molecules adsorbed on catalyst. Since the overall rates are dependent on the partial pressures of CH_3OH and O_2, the reaction between the adsorbed methanol and oxygen is the rate-determining step in the overall reaction rate as follows;

$$CH_3OH \rightleftharpoons (CH_3OH)_{ad}, \quad (4)$$

$$\tfrac{1}{2}O_2 \rightleftharpoons O_{ad}, \quad (5)$$

$$(CH_3OH)_{ad} + O_{ad} \rightarrow \text{Products}. \quad (6)$$

The conductivity data in Fig. 4 indicate that the adsorption of methanol is essentially ionic. Therefore, one can write the reasonable equilibrium:

$$(CH_3OH)_{ad} \rightleftharpoons (CH_3OH)_{ad}^{+} + e^{-}. \quad (7)$$

It seems that the fast dissociation of $(CH_3OH)_{ad}^{+}$ takes place subsequently according to the following equilibrium similar to the results for the catalytic decomposition of methanol on Ni foils (*13*):

$$(CH_3OH)_{ad}^{+} + e^{-} \rightleftharpoons (CH_3O)_{ad}^{+} + H_{ad}^{+} + 2e^{-}. \quad (8)$$

Moreover, $(CH_3O)_{ad}^{+}$ is decomposed to such adsorbed species as CH_2O^{+} or CO^{+} (*13*). CO and H_2, however, could not be detected in outlet gases under the experimental conditions. Thus, the reaction between other species and adsorbed oxygen is extremely fast. According to Eq. (7) or (8), the electron which is produced in the process of ionization would be competing with the concentration of conduction electrons in $LnFeO_3$.

Meanwhile, a conduction electron is produced by the following equilibrium in a manner similar to that for α-Fe_2O_3 (*14*):

$$n\,O_L^{2-} \rightleftharpoons n/2\,O_2 + 2n\,e^{-} + nV_o. \quad (9)$$

In equilibrium (9), V_o is an oxygen vacancy, e^{-} is a conduction electron, O_L^{2-} is a lattice oxygen in $LnFeO_3$. Equation (9) means that the number of conduction electrons varies with the partial pressure of oxygen in the gas phase. Under the condition of which the equilibrium (9) proceeds to the right, the difference of ionic strength for Fe–O bond among $LnFeO_3$ would affect the facility of evolution of lattice oxygen to gas phase. The experimental data shown in Fig. 4 show that the magnitude of the conductivity change decreases with increasing O_2 concentration in carrier gas. This result indicates that the excess methanol consumes the lattice oxygen in $LnFeO_3$ and the conduction electron increases. Thus, if the amount of pulsed methanol is consistent with the oxygen concentration in which the methanol oxidation reaction proceeds stoichiometrically, the conductivity change due to the injection of methanol would not apparently appear. Therefore, the conductivity change above 2.0 vol% of oxygen concentration may be attributed to the rise of temperature on thin film under the complete oxidation of methanol.

On the other hand, it would seem that the electron in Eq. (7) or (8) is used for the activation of adsorbed oxygen under the steady-state reaction as follows:

$$O_{ad} + e^{-} \rightleftharpoons O_{ad}^{-}, \quad (10)$$

$$O_{ad} + 2e^{-} \rightleftharpoons O_{ad}^{2-}. \quad (11)$$

Thus, an adsorbed oxygen can easily react with $(CH_3OH)_{ad}^{+}$ or $(CH_3O)_{ad}^{+}$ and H_{ad}^{+} according to the following equations:

$$(CH_3OH)_{ad}^{+} + O_{ad}^{-} \rightarrow \text{Products} \quad (12)$$

or

$$(CH_3O)_{ad}^{+} + H_{ad}^{+} + O_{ad}^{2-} \rightarrow \text{Products}. \quad (13)$$

Since the activity of $LnFeO_3$ is correlated with the ionic strength of Fe–O bond, it appears that adsorbed oxygen and lattice oxygen in $LnFeO_3$ attain equilibrium fairly rapidly at reaction temperature as given by Eq. (14).

$$O_{ad}^{2-} \rightleftharpoons O_L^{2-}. \quad (14)$$

Therefore, the oxidation of methanol on $LnFeO_3$ under the steady state would mainly proceed according to Eq. (13) as the

rate-determining step. However, the reaction path to the final products H_2O and CO_2 seems to be very complex.

ACKNOWLEDGMENT

The authors are happy to acknowledge the support of a Scientific Research Grant from the Ministry of Education, Japan, for part of this work.

REFERENCES

1. Obayashi, H., Sakurai, Y., and Gojo, T., *J. Solid State Chem.* **17,** 299 (1976).
2. Vogel, E. M., Johnson, D. W., Jr., and Gallagher, P. K., *J. Amer. Ceram. Soc.* **60,** 31 (1977).
3. Voorhoeve, R. J. H., Johnson, D. W., Jr., Remeika, J. P., and Gallagher, P. K., *Science* **195,** 827 (1977).
4. Arakawa, T., Takeda, S., Adachi, G., and Shiokawa, J., *Mater. Res. Bull.* **14,** 507 (1979).
5. Arakawa, T., Adachi, G., and Shiokawa, J., *Nippon Kagaku Kaishi* **1980,** 1573 (1980).
6. Arakawa, T., Yoshida, A., and Shiokawa, J., *Mater. Res. Bull.* **15,** 269 (1980).
7. Arakawa, T., Yoshida, A., and Shiokawa, J., *Mater. Res. Bull.* **15,** 347 (1980).
8. Arakawa, T., Tsuchi-ya, S., and Shiokawa, J., *Mater. Res. Bull.* **16,** 97 (1981).
9. Treves, D., *J. Appl. Phys.* **36,** 1033 (1965).
10. Jørgensen, C. K., and Berthou, H., *Faraday Discuss. Chem. Soc.* **54,** 269 (1972).
11. Gelius, U., Heden, P. F., Hedman, J., Lindberg, B. J., Manne, R., Nordberg, R., Nordling, C., and Siegbahn, K., *Phys. Scr.* **2,** 70 (1970).
12. Carver, J. C., Schweitzer, G. K., and Carlson, T. A., *J. Chem. Phys.* **57,** 973 (1972).
13. Steinbach, F., Spengler, H. J., Bohlmann, H. J., and Hynding, J., *in* "Proceedings, 7th International Congress on Catalysis, 1981," p. 122.
14. Kim, K. H., Han, H. S., and Choi, J. S., *J. Chem. Phys.* **83,** 1286 (1979).